

Hesperidin Induces Mitochondria Mediated Intrinsic Apoptosis in HPV-positive Cervical Cancer Cells via Regulation of E6/p53 Expression

Fang Ren (✉ ren.fang@yahoo.com)

Zhengzhou University <https://orcid.org/0000-0003-3971-1072>

Gong Zhang

Zhengzhou University

Caiyu Li

Zhengzhou University

Gailing Li

Zhengzhou University

Yuan Cao

Zhengzhou University

Fangfang Sun

Zhengzhou University

Primary research

Keywords: Human papilloma virus (HPV)-positive cervical cancer cells, Hesperidin, Apoptosis, Mitochondria-mediated intrinsic pathway, E6, p53

Posted Date: November 13th, 2020

DOI: <https://doi.org/10.21203/rs.3.rs-105340/v1>

License: © ⓘ This work is licensed under a Creative Commons Attribution 4.0 International License.

[Read Full License](#)

Abstract

Background: Hesperetin, an active compound found in citrus fruits, possesses antiproliferative effects toward several types of cancer cell lines, including cervical cancer. In this study, we explore the antitumor effects of Hesperetin on the human cervical cancer human papilloma virus (HPV)-positive (CaSki and HeLa) and HPV-negative (C-33A) cell lines and further elucidated the underlying mechanisms of this action.

Methods: Cell viability and proliferation was measured by the MTT assay and 5-ethynyl-2'-deoxyuridine (EdU) incorporation assay, respectively. dUTP-fluorescein nick end-labeling (TUNEL) staining, Annexin V-fluorescein isothiocyanate (FITC)/propidium iodide (PI) staining and flow cytometry was used to assess the degree of apoptosis. JC-1 staining assay was used to evaluate the change of mitochondrial membrane potential ($\Delta\Psi_m$) and Western blot assays were used to determine apoptosis-related factors at protein level.

Results: Hesperetin (100, 200 and 400 μM) exhibited a significant exclusive inhibitory effect against the growth of HPV-infected CaSki and HeLa cancer cells via induction of apoptosis in a concentration-dependent manner, while it was almost not active in HPV-negative C-33A cancer cells and normal cervix epithelial H8 cells. Moreover, this antitumor effect executed by Hesperetin was associated with disruption of $\Delta\Psi_m$, the release of cytochrome c from mitochondria, activation of pro-apoptotic proteins (Bax, cleaved caspase-3 and caspase-9) and inhibition of anti-apoptotic proteins (Bcl-2). During this process, cleaved caspase-8 remained unchanged. In addition, Hesperetin led to a downregulation of E6 oncoprotein expression and upregulation of tumor suppressor protein p53 level.

Conclusions: Collectively, these results implicated that Hesperetin can induce apoptosis of HPV-positive cervical cancer cells via a mitochondria-mediated intrinsic signaling pathway, together with the repression of E6 and enhancement of p53 protein level, indicating Hesperetin may be considered as a potential candidate for the development of innovative anti-HPV cervical cancer agents.

Introduction

Cervical cancer is one of common malignant neoplasm in women worldwide, second to breast cancer, which is closely related to human papilloma virus (HPV) persistent infection [1, 2]. Among 15 HPV subtypes, responsible for invasive cervical cancer [2], HPV16 and 18 account for at least 70% of all cervical cancer cases [3]. Although current therapeutic strategies for cervical cancer (i.e., surgery, radiotherapy, and chemotherapy or their combination) have alleviated its progression to a refractory form, they work with limited value in patients with advanced or recurrent cervical cancer. However, 5-year overall survival rates with this treatment are about only 50% [4]. Two new incoming HPV vaccines, such as Cervarix® or Gardasil®, only fight for a small fraction of HPV types-associated cervical lesions, but the cost of vaccination programs put a heavy burden for developing countries [5, 6]. Despite advances in the therapy of this disease, multiple chemotherapeutic resistance, the poor prognosis and undesirable

side-effects promoted many researchers to explore novel chemotherapeutic agents for this type of cancer.

In recent years, plant-derived natural products has become rich gold mines for seeking more effective and less toxic anti-cancer agents, due to their multi-target, multi-link and multichannel antitumor effects [7, 8]. This greatly expedites drug discovery of special virus inhibitors to fight against HPV-associated cervical cancer. Hesperetin, the glycoside ligand derivative of hesperetin, occurs abundantly in citrus fruits, which possesses various biological and pharmacological activities, such as antioxidant, anti-inflammatory, antihypertensive, and anti-atherogenic properties [9, 10]. Emerging evidence has also suggested that this bioactive natural product has received considerable attention, due to its anti-carcinogenic activities in various types of cancer cells, including gastric cancer, colon cancer, hepatocellular cancer, breast cancer, lung cancer, renal cancer, oral cancer, prostate cancer and cervical cancer cells [11–13]. Alshatwi et al portrayed that Hesperetin exhibited a potential anticancer activity against HPV16 positive SiHa cervical cancer cell line in vitro through induction of both death receptor– and mitochondria-mediated apoptosis. Another in vitro study conducted by Prakash et al highlighted the hesperetin showed noteworthy tumor growth inhibitory effect on HeLa cells in vitro and the molecular docking analysis predicted that a strong binding interaction between hesperetin and the active site of E6 protein of HPV16 cervical carcinoma [14]. However, related studies elucidating the role and the mechanism(s) of action of Hesperetin in cervical cancer are not well fully understood. Accordingly, the present study was performed to validate if HPV-type selectivity of Hesperetin can be observed in other cervical cancer cell lines containing HPV 16 and 18 and to clarify the possible molecular mechanism involved in this anti-carcinogenic activity.

Materials And Methods

Materials and chemicals

Hesperidin (purity $\geq 98\%$) and 3-(4, 5-dimethylthiazol-2-yl)-2, 5-diphenyltetrazolium bromide (MTT) were supplied by Sigma Aldrich (St. Louis, MO, USA). Antibodies against Bax, Bcl-2, cleaved-caspase-3, cleaved-caspase-8, cleaved-caspase-9, E6, p53, β -actin and horseradish peroxidase (HRP)-linked secondary antibody were from Santa Cruz Biotechnology (Santa Cruz, CA, USA). 5,5',6,6'-tetrachloro-1,1',3,3'-tetraethylbenzimidazolylcarbocyanine iodide (JC-1), Dulbecco's modified Eagle's medium (DMEM), and fetal bovine serum (FBS) penicillin, and streptomycin were obtained from Invitrogen (Carlsbad, CA, USA). Pharmingen (San Diego, CA, USA). dUTP-fluorescein nick end-labeling (TUNEL) assay kit from Nanjing Jiancheng Bioengineering Institute (Nanjing, China). Annexin V-fluorescein isothiocyanate (FITC)/propidium iodide (PI) kit was from BD Biosciences (San Jose, CA, USA). All the other chemicals used were of analytical grade commercially available.

Cell culture

The human cervical cancer cell lines CaSki (HPV 16 positive), HeLa (HPV 18 positive), C-33A (HPV negative) and normal cervix epithelial H8 cells were purchased from Shanghai Institute of Biochemistry and Cell Biology cell Bank (Shanghai, PR China) and cultured in Dulbecco's modified Eagle's medium

(DMEM) supplemented with 10% heat-inactivated 10% FBS, 2 mM L-glutamine, 100 U/ml penicillin G and 100 mg/ml streptomycin at 37 °C in a humidified atmosphere containing 5% CO₂ .at 37 °C

MTT assay

Cells viability was analyzed using MTT assay, which is based on the conversion of MTT to formazan crystals by mitochondrial dehydrogenases [15]. Briefly, exponentially growing cancer cells at a density of 1×10^4 cells/well in 96-well plates were treated with different concentrations of Hesperetin for 24, 48 and 72 h. Then, 20 µl MTT solutions (5 mg/ml) was added and incubated for 4 h. The medium containing MTT was removed and 100 µl DMSO was added to each well to dissolve the purple coloured formazan crystals. Finally, Absorbance was read at 570 nm (630 nm as a reference) on a microplate reader (Bio-Rad, Tokyo, Japan). The cell viability values were calculated as follows: the ratio of cell survival (%) = $(\text{mean Absorbance}_{\text{sample}} - \text{mean absorbance}_{\text{blank}}) / (\text{mean Absorbance}_{\text{control}} - \text{mean absorbance}_{\text{blank}}) \times 100$.

5-ethynyl-2'-deoxyuridine (EdU) incorporation assay

EdU staining kit was employed to assess the cells proliferation. Briefly, different treated cells were washed with ice cold PBS and fixed in 4% freshly prepared formaldehyde in PBS for 20 min at 37 °C. After that cells were washed with ice cold PBS, the cells were stained with EdU staining kit in accordance with manufacturer's instructions. Finally, the stained cells were further washed with PBS and were photographed under a fluorescence microscope (Agilent 1200; Agilent Technologies).

TUNEL assay

Apoptotic cell death was performed by TUNEL assay kit as per the manufacturer's protocols. Briefly, following different treatment, cells on cover slips were washed with ice cold PBS and fixed in 4% freshly prepared paraformaldehyde. After 15 min, fixed cells were washed with PBS and permeabilized in PBS containing 0.1% Triton X-100 at 37 °C for 2 min. Thereafter, the cells were stained with TUNEL reaction mixture in the dark at 37 °C for 1 h and then washed with PBS, followed by the addition of 100 µl of DAPI (1 µg/ml) to stain nuclei. Finally, image acquisitions were performed by a fluorescent microscope (Nikon ECLIPSE 80i, Tokyo, Japan). The apoptotic index was expressed as the percentage of apoptotic cells (TUNEL-positive) compared to total cells (DAPI-positive). Five randomly selected microscopic fields in each group were used to calculate the apoptotic index and all the experiments were performed three times.

Flow cytometric analysis using Annexin V-FITC/PI double staining

The percentage of apoptotic cells was evaluated by using an Annexin V-FITC Apoptosis Detection Kit according to the manufacturer's instructions. In brief, treated cells were harvested and washed with ice cold PBS. After centrifugation, the resulting cell pellet was resuspended in 500 µl binding buffer followed by addition of 5 µl of Annexin V-FITC conjugate and 10 µl of PI for at least 20 min incubation at room temperature in the dark. Finally, the sample was immediately subjected to FACSCalibur flow cytometer

(Becton-Dickinson, Mansfield, MA, USA) and each measurement was performed at least using 1×10^4 cells with CellQuest software (BD Biosciences) for data analysis. Annexin V and PI negative represents viable cells; annexin V positive and PI negative represents early apoptotic cells; annexin V negative, PI-positive represents necrotic cells and annexin V positive and PI positive late represents apoptotic cells. The experiments were repeated for three times.

Measurement of mitochondrial membrane potential ($\Delta\Psi_m$)

Measurement of $\Delta\Psi_m$ change in cancer cells was performed using JC-1 dye at an excitation wavelength of 480 nm and emission wavelengths of 530 nm (red, maintained $\Delta\Psi_m$) and 590 nm (green, disrupted $\Delta\Psi_m$). The ratio of green fluorescence at 530 nm to red fluorescence at 590 nm is directly related to $\Delta\Psi_m$ [16]. Briefly, cancer cells (2×10^6 cells/ml) were seeded in 6-well plate and subjected to incubation for 48 h at 37 °C. Then, the cells were collected, washed with PBS and stained with JC-1 staining solution (5 µg/mL) for 30 min at 37 °C in the dark. The stained cells were washed again with PBS and images were immediately acquired under an inverted fluorescence microscope (Leica, Wetzlar, Germany). The intensity of green to red fluorescence was measured by Image J software.

Western blot assay

After treatment, the cells were washed twice in cold PBS, collected and lysed in RIPA lysis buffer on ice. The resulting cellular lysates were subjected to centrifugation at $14,000 \times g$ for 5 min and supernatant fractions were collected for protein qualification with BCA protein assay kit. Samples with 50 µg of total protein were separated by 0% SDS-PAGE gels and transferred to polyvinylidene difluoride (PVDF) membrane. The membranes were then blocked with 5% skim milk in TBST for 1–2 h at room temperature, probed with primary antibody against cytochrome c, Bax, Bcl-2, cleaved caspae-3, E6, P53 and Rb overnight at 4 °C, and then incubated with horseradish-peroxidase (HRP)-conjugated secondary antibodies at 37°C for 1 h. Finally, bands of specific proteins were developed using an enhanced chemiluminescent detection system (Pierce Biotechnology Inc., Rockford, IL) and the band intensity was analyzed with an Image-Pro Plus v6.0 software (Media Cybernetics, USA) normalized to an internal control protein β -actin.

Statistical analysis

Results were expressed as the mean \pm standard deviation (S.D.) of three independent assays. The statistical differences were compared using One-way analysis of variance (ANOVA) and Student's t test. All statistical analyses were performed using GraphPad Prism 6.0 software. A value of $P < 0.05$ was considered significant.

Results And Discussion

The effects of Hesperidin on the cell viability and proliferation of CaSki, HeLa, C-33A and epithelial H8 cells

To examine the cytotoxic effects of Hesperidin in different type of cervical cancer cells, HPV 16 positive CaSki cells, HPV 18 positive HeLa cells, HPV negative C-33A cells and normal cervix epithelial H8 cells were exposed to increasing doses of Hesperidin (25, 50, 100, 200 and 400 μ M) for 24 h, 48 h and 72 h. Following this treatment, the cytotoxic effects and antiproliferative effect of Hesperidin on difference cells were assessed using the MTT assay and EdU incorporation assay, respectively. It was showed in Fig. 1A-D that cell viability of CaSki and HeLa cells was inhibited after exposure to Hesperidin in a time- and concentration-dependent manner, which was significantly different from untreated control especially at the concentration of 100, 200 and 400 μ M of Hesperidin at 48 h ($P < 0.05$, $P < 0.01$). Only a moderate inhibitory effect can be observed in C-33A cells in response to Hesperidin treatment at the highest concentration of 400 μ M at 72 h when compared with control cells ($P < 0.05$). In contrast, cell viability of H8 cells kept still unchanged in all experiments ($P > 0.05$). Supporting this result, EdU incorporation assay revealed lower green fluorescence intensity in CaSki and HeLa cancer cells treated with Hesperidin (100, 200 and 400 μ M) for 48 h (Fig. 2A and B). The results suggested that Hesperidin inhibited the growth of CaSki and HeLa cancer cells more effectively than that of C-33A and non-cancer cells.

The effects of Hesperidin on the apoptosis of CaSki and HeLa cells

Next, we investigate if this cell growth inhibition induced by Hesperidin was related to apoptosis using TUNEL staining and annexin V-FITC/PI staining assay based on flow cytometry. It was clear that number of cells with purplish red stained TUNEL-positive nuclei was increased in both cervical cancer cell lines upon treatment with Hesperidin (100, 200 and 400 μ M) when compared with untreated control group (Fig. 3A and B). Concurrently, the percentage of Annexin V-positive cells, namely the early apoptosis (Annexin V⁺ and PI⁻) and late apoptosis cells (Annexin V⁺ and PI⁺), was upregulated in cancer cells in response to treatment with Hesperidin for 48 h in a concentration-dependent manner (Fig. 4A and B). The apoptosis rate is 18.5%, 23.6% and 46.3% for Hesperidin-treated CaSki cells, and 18.8%, 29.3% and 51.3% for Hesperidin-treated HeLa cells at respective concentration of 100, 200 and 400 μ M. In addition, only a small amount of apoptotic and dead cells was observed in control group. This result indicated that Hesperidin can induce apoptosis of both HPV-positive cervical cancer cells.

The effects of Hesperidin on the mitochondrial membrane potential change of CaSki and HeLa cells

To assess if Hesperidin-induced cell apoptosis in both HPV-positive cervical cancer cells is implicated with the depletion of MMP, the change of MMP was analyzed by employing JC-1 dye and flow cytometry (Fig. 5A and B). Fluorescence microscopy result showed bright red fluorescence in untreated control cells. With the addition of Hesperidin (100, 200 and 400 μ M), red fluorescence signals became decreased, but green fluorescence signals turned strong in CaSki and HeLa cancer cells. The ratio of red/green fluorescence detected by flow cytometry are 1.61, 0.67 and 0.37 in CaSki cells treated Hesperidin at the concentration of 100, 200 and 400 μ M, and 1.71, 0.45 and 0.23 in HeLa cells treated Hesperidin at the

concentration of 100, 200 and 400 μM , respectively. The fluorescence signal change from red to green indicated that Hesperidin can cause severe disruption of MMP.

The effects of Hesperidin on the cytochrome c, Bcl-2 and caspases family proteins expression of CaSki and HeLa cells

Due to the direct role of mitochondria in Hesperidin-induced apoptosis, we next perform Western blotting using specific antibodies as indicated to investigate mitochondrial-related apoptotic proteins, such as cytosolic cytochrome c, Bax, Bcl-2, cleaved caspase-3, cleaved caspase-8, and cleaved caspase-9. As shown in Fig. 6A and B, Hesperidin addition (100, 200 and 400 μM) resulted in a dose-dependent increased expression of cytosolic cytochrome c, Bax, cleaved caspase-3, and cleaved caspase-9, but a significant decrease of Bcl-2 in the Hesperidin-treated AGS CaSki and HeLa cells. However, cleaved caspase-8 protein expression remained same as in control cells. These results suggest mitochondria-mediated (intrinsic) pathway played an important role in Hesperidin induced apoptosis for both cervical cancer cells.

The effects of Hesperidin on the HPV E6 and p53 expression of CaSki and HeLa cells

Since selective toxicity of Hesperidin to HPV-positive cervical cancer cells, the expression of the E6 protein was examined in both cancer cells by performing Western blotting. Figure 7A and B typically showed that treatment with Hesperidin at the concentration of 100, 200 and 400 μM for 48 h resulted in a concentration-dependent downregulation of E6 oncoproteins, but an upregulation of p53 tumor suppressor protein in CaSki and HeLa cells, suggesting HPV E6 and p53 may be the key target of antitumor action of Hesperidin toward HPV-positive cervical cancer cells.

Discussion

Searching natural product from medicinal plants with tumor growth inhibitory activity and less toxicity has become a continuous effort in the prevention and treatment of cancer, including HPV-infected cervical cancer [17, 18]. In the present study, we first investigated the cytotoxic and antiproliferative effects of Hesperidin on different type of cervical cancer cells, including HPV 16 positive CaSki cells, HPV 18 positive HeLa cells and HPV negative C-33A cells, and on normal cervix epithelial H8 cells. MTT assay clearly demonstrated that Hesperidin (100, 200 and 400 μM) treatment significantly inhibited the viability of HeLa and SiHa cells, and its inhibition rate also increased with the concentration of Hesperidin and indicated time periods. However, no marked inhibitory effect was observed in C-33A cells except at the highest concentration of Hesperidin (400 μM) after 72 h and cell viability of normal cervix epithelial H8 cells remained unchanged in all Hesperidin-treated groups as compared with untreated control ($P > 0.05$).

In line with this result, EdU incorporation assay demonstrated the similar tendency for antiproliferative effects of Hesperidin on these cells as same as cell viability in MTT assay. The green fluorescence intensity was decreased in CaSki and HeLa cancer cells following treatment with Hesperidin (100, 200 and 400 μ M) for 48 h in a concentration-dependent manner. Based on these results, we can presume that Hesperidin might be a promising antitumor drug to treat HPV positive type cervical cancer.

Considering this decreased cell viability and proliferation of Hesperidin-treated cervical cancer cells in the presence of Hesperidin, we next examine if apoptosis induction by Hesperidin was involved in this effect. TUNEL staining assay portrayed that the addition of Hesperidin resulted in an increased cells with purplish red stained TUNEL-positive nuclei visualized by a fluorescent microscope. Supporting this observing, Annexin V-FITC/PI double staining result on flow cytometry further confirmed that Hesperidin supplement evoked a high apoptosis rate of CaSki and HeLa cancer cells in a dose-dependent manner when compared with untreated control cells. These results confirmed that the cell growth inhibitory of Hesperidin on CaSki or HeLa cells was achieved by induction of apoptosis

Apoptosis or programmed cell death is triggered by two main types of signal pathways, namely death receptor-mediated (extrinsic) and mitochondria-mediated (intrinsic) pathway [19]. The mitochondria working as the cross-talk organelles can connect both the extrinsic and intrinsic apoptotic pathways [20]. It is well known that the loss of mitochondrial membrane potential ($\Delta\Psi$ m) played an important role in the initiation of early mitochondrial-related apoptosis [21], and thus we measured the change in $\Delta\Psi$ m in cervical cancer cells induced by Hesperidin using JC-1 dye. In healthy cells, JC-1 aggregates in mitochondria where JC-1 dimmers emits a red fluorescence at 590 nm, whereas JC-1 monomers in the cytosol exhibits green fluorescence at 530 nm attributable to the mitochondrial depolarization [22]. Once the MMP decreased, JC-1 fluorescence color will shift from red fluorescence to green. Thereafter, the relative low ratio of the red/green fluorescence indicated the collapse of MMP. Fluorescence microscopy demonstrated that a reduced red fluorescence signals, but an increased green fluorescence signals in CaSki cells and HeLa cells following treatment with Hesperidin for 48 h, suggesting a MMP loss upon Hesperidin treatment.

Experimental evidence suggests that the mitochondria-mediated intrinsic and receptor-mediated extrinsic apoptosis pathways can be differentiated by involvement of initiator caspase-8 or -9, respectively [23]. Once the activation of caspase-8 or -9, both intrinsic and extrinsic pathways would trigger the common executioner caspases (caspase-3 and caspase-7) to execute apoptosis [24, 25]. During mitochondria-mediated intrinsic apoptosis pathway, Bcl-2 family proteins work as critical regulators of mitochondrial membrane permeability and consist of pro- (Bax and Bak) and anti-apoptotic (Bcl-2 and Bcl-xL) members, which form heterodimers to inhibit or activate each other [26]. The rise of ratio between pro-apoptotic protein Bax and anti-apoptotic protein Bcl-2 can induce mitochondrial damage and then cause the release of cytochrome c from mitochondria to the cytoplasm where cytochrome c forms apoptosome complex with AIF to subsequently activate caspase-9 as well as downstream effector caspase-3, thus inducing apoptosis [27]. Due to the MMP collapse, we further investigated the mitochondrial-related apoptotic proteins, including cytosolic cytochrome c, Bax, Bcl-2, cleaved caspase-3, cleaved caspase-8, and cleaved

caspase-9. The expression levels of cytosolic cytochrome c, Bax, cleaved caspase-3, and cleaved caspase-9 protein were significantly increased in a dose-dependent manner in CaSki and HeLa cells upon Hesperidin treatment. In contrast, the expression level of Bcl-2 was decreased in both cells following Hesperidin treatment (Fig. 3B). Cleaved caspase-8 protein expression kept unchanged as control. These results suggested that Hesperidin treatment induced apoptosis of CaSki and HeLa cells via a mitochondria-mediated (intrinsic) pathway.

Mitochondria-mediated apoptosis involves not only the activation of caspase-9-dependent intrinsic pathway but also p53-related signaling molecules [28]. HPV encoded viral oncoprotein E6 is essential for cervical carcinogenesis by its potential to inactivate the tumor suppressor proteins p53, which plays an important role in the regulation of cell cycle and apoptosis [39 – 31]. Hence p53 served as tumor suppression element in multicellular organisms to suppress cancer and its defectiveness would allow abnormal cells to proliferate, resulting in cancer. It was evident that Hesperidin concentration-dependently decreased the expression of E6 oncoprotein in CaSki and HeLa cells, but increased tumor suppressor protein p53. All these results suggested that the expression of decreased HPV E6 and increased p53 protein were involved in the antitumor effect of Hesperidin toward CaSki and HeLa cells.

Conclusion

In summary, the present findings suggested for the first time that Hesperidin was able to inhibit the proliferation and induce cells apoptosis of HPV-infected cervical cancer cells via mitochondria dependent intrinsic apoptosis pathway accompanying with E6 repression and p53 cascades enhancement. Therefore, our results provide strong rooting for the notion that Hesperidin might be helpful in developing a novel chemotherapeutics candidate in treatment of HPV-infected cervical cancer. Further intensive preclinical and clinical studies are also highly required in progress before its clinical application.

Abbreviations

HPV: Hhuman papilloma virus; EdU: 5-ethynyl-2'-deoxyuridine; TUNEL : dUTP-fluorescein nick end-labeling; MTT: 3-(4, 5-dimethylthiazol-2-yl)-2, 5-diphenyltetrazolium bromide; JC-1: 5,5',6,6'-tetrachloro-1,1',3,3'-tetraethylbenzimidazolylcarbocyanine iodide; DMEM: Dulbecco's modified Eagle's medium; FBS: fetal bovine serum; Annexin V – FITC/PI: Annexin V-fluorescein isothiocyanate /propidium iodide; PVDF: Polyvinylidene difluoride; HRP: Horseradish-peroxidase

Declarations

Ethics approval and consent to participate

Not applicable.

Consent for publication

All authors read and approved the final manuscript.

Availability of data and materials

All data generated or analyzed during this study are included in this published article.

Competing interests

The authors declare that they have no competing interests.

Funding

Not applicable.

Authors' contributions

FR and GZ designed the experiments, performed the research and analyzed the data. FR, GZ, CL, GL, YC and FS performed the cell culture and western blots. GL, YC and FS performed the literature research and data analysis. FR wrote and revised the manuscript. All authors read and approved the final manuscript.

Acknowledgements

Not applicable.

References

1. Li GL, et al. HPV E6 down-regulation and apoptosis induction of human cervical cancer cells by a novel lipid-soluble extract (PE) from *Pinellia pedatisecta* Schott in vitro. *J Ethnopharmacol.* 2010;132(1):56-64.
2. Marcela GM, Eva RG, Del Carmen RM, Rosalva ME. Evaluation of the Antioxidant and Antiproliferative Effects of Three Peptide Fractions of Germinated Soybeans on Breast and Cervical Cancer Cell Lines. *Plant Foods Hum Nutr.* 2016;71(4):368-74.
3. Hirchaud F, et al. Isoliquiritigenin induces caspase-dependent apoptosis via downregulation of HPV16 E6 expression in cervical cancer Ca Ski cells. *Planta Med.* 2013;79(17):1628-35.
4. Hougardy BM, Maduro JH, van der Zee AG, Willemse PH, de Jong S, de Vries EG. Clinical potential of inhibitors of survival pathways and activators of apoptotic pathways in treatment of cervical cancer: changing the apoptotic balance. *Lancet Oncol.* 2005;6(8):589-98.
5. Stanley M. Potential mechanisms for HPV vaccine-induced long-term protection. *Gynecol Oncol.* 2010;118(1 Suppl):S2-7.
6. Pogoda CS, Roden RB, Garcea RL. Immunizing against Anogenital Cancer: HPV Vaccines. *PLoS Pathog.* 2016;12(5):e1005587. Published 2016 May 19.

7. Deng H, et al. Identification of fluorinases from *Streptomyces* sp MA37, *Nocardia brasiliensis*, and *Actinoplanes* sp N902-109 by genome mining. *Chembiochem*. 2014;15(3):364-8.
8. Ma L, et al. Discovery of Myricetin as a Potent Inhibitor of Human Flap Endonuclease 1, Which Potentially Can Be Used as Sensitizing Agent against HT-29 Human Colon Cancer Cells. *J Agric Food Chem*. 2019;67(6):1656-65.
9. Zhang J, et al. Hesperetin Induces the Apoptosis of Gastric Cancer Cells via Activating Mitochondrial Pathway by Increasing Reactive Oxygen Species. *Dig Dis Sci*. 2015;60(10):2985-95.
10. Wu D, et al. Hesperetin inhibits Eca-109 cell proliferation and invasion by suppressing the PI3K/AKT signaling pathway and synergistically enhances the anti-tumor effect of 5-fluorouracil on esophageal cancer in vitro and in vivo. *RSC Adv*. 2018;8(43): 24434-43.
11. Roohbakhsh A, Parhiz H, Soltani F, Rezaee R, Iranshahi M. Molecular mechanisms behind the biological effects of hesperidin and hesperetin for the prevention of cancer and cardiovascular diseases. *Life Sci*. 2015;124:64-74.
12. Ferreira de Oliveira JMP, Santos C, Fernandes E. Therapeutic potential of hesperidin and its aglycone hesperetin: Cell cycle regulation and apoptosis induction in cancer models. *Phytomedicine*. 2020;73:152887.
13. Zhang J, et al. Hesperetin Induces the Apoptosis of Gastric Cancer Cells via Activating Mitochondrial Pathway by Increasing Reactive Oxygen Species. *Dig Dis Sci*. 2015;60(10):2985-95.
14. Prakash S, et al. Isolation of hesperetin-A flavonoid from *Cordia sebestena* flower extract through antioxidant assay guided method and its antibacterial, anticancer effect on cervical cancer via in vitro and in silico molecular docking studies. *J Mol Struct*. 2020;1207: 127751.
15. Mosmann T. Rapid colorimetric assay for cellular growth and survival: application to proliferation and cytotoxicity assays. *J Immunol Methods*. 1983;65(1-2):55-63.
16. Yao W, et al. Delicaflavone induces apoptosis via mitochondrial pathway accompanying G2/M cycle arrest and inhibition of MAPK signaling cascades in cervical cancer HeLa cells. *Phytomedicine*. 2019;62:152973.
17. Wang SJ, et al. Plants and cervical cancer: an overview. *Expert Opin Investig Drugs*. 2013;22(9):1133-56.
18. Zaman MS, Chauhan N, Yallapu MM, et al. Curcumin Nanoformulation for Cervical Cancer Treatment. *Sci Rep*. 2016;6:20051.
19. Zhou X, Jiang W, Liu Z, Liu S, Liang X. Virus Infection and Death Receptor-Mediated Apoptosis. *Viruses*. 2017;9(11):316.
20. López-Hernández FJ, Ortiz MA, Piedrafita FJ. The extrinsic and intrinsic apoptotic pathways are differentially affected by temperature upstream of mitochondrial damage. *Apoptosis*. 2006;11(8):1339-47.
21. Taneja N, Tjalkens R, Philbert MA, Rehemtulla A. Irradiation of mitochondria initiates apoptosis in a cell free system. *Oncogene*. 2001;20(2):167-77.

22. Li C, Wang Y, Wang C, Yi X, Li M, He X. Anticancer activities of harmine by inducing a pro-death autophagy and apoptosis in human gastric cancer cells. *Phytomedicine*. 2017;28:10-18.
23. Yu HY, et al. β -lapachone-Induced Apoptosis of Human Gastric Carcinoma AGS Cells Is Caspase-Dependent and Regulated by the PI3K/Akt Pathway. *Biomol Ther (Seoul)*. 2014;22(3):184-92.
24. Chowdhury I, Tharakan B, Bhat GK. Current concepts in apoptosis: the physiological suicide program revisited. *Cell Mol Biol Lett*. 2006;11(4):506-25.
25. Elmore S. Apoptosis: a review of programmed cell death. *Toxicol Pathol*. 2007;35(4):495-516.
26. Aouacheria A, Cibiel A, Guillemin Y, Gillet G, Lalle P. Modulating mitochondria-mediated apoptotic cell death through targeting of Bcl-2 family proteins. *Recent Pat DNA Gene Seq*. 2007;1(1):43-61.
27. Song W, et al. Polysaccharide-induced apoptosis in H22 cells through G2/M arrest and BCL2/BAX caspase-activated Fas pathway. *Cell Mol Biol (Noisy-le-grand)*. 2015;61(7):88-95.
28. Koh DW, Dawson TM, Dawson VL. Mediation of cell death by poly(ADP-ribose) polymerase-1. *Pharmacol Res*. 2005;52(1):5-14.
29. zur Hausen H. Papillomavirus infections—a major cause of human cancers. *Biochim Biophys Acta*. 1996;1288(2):F55-F78.
30. Hong B, van den Heuvel AP, Prabhu VV, Zhang S, El-Deiry WS. Targeting tumor suppressor p53 for cancer therapy: strategies, challenges and opportunities. *Curr Drug Targets*. 2014;15(1):80-9.
31. Yan L, et al. Involvement of p53-dependent apoptosis signal in antitumor effect of Colchicine on human papilloma virus (HPV)-positive human cervical cancer cells. *Biosci Rep*. 2020;40(3):BSR20194065.

Figures

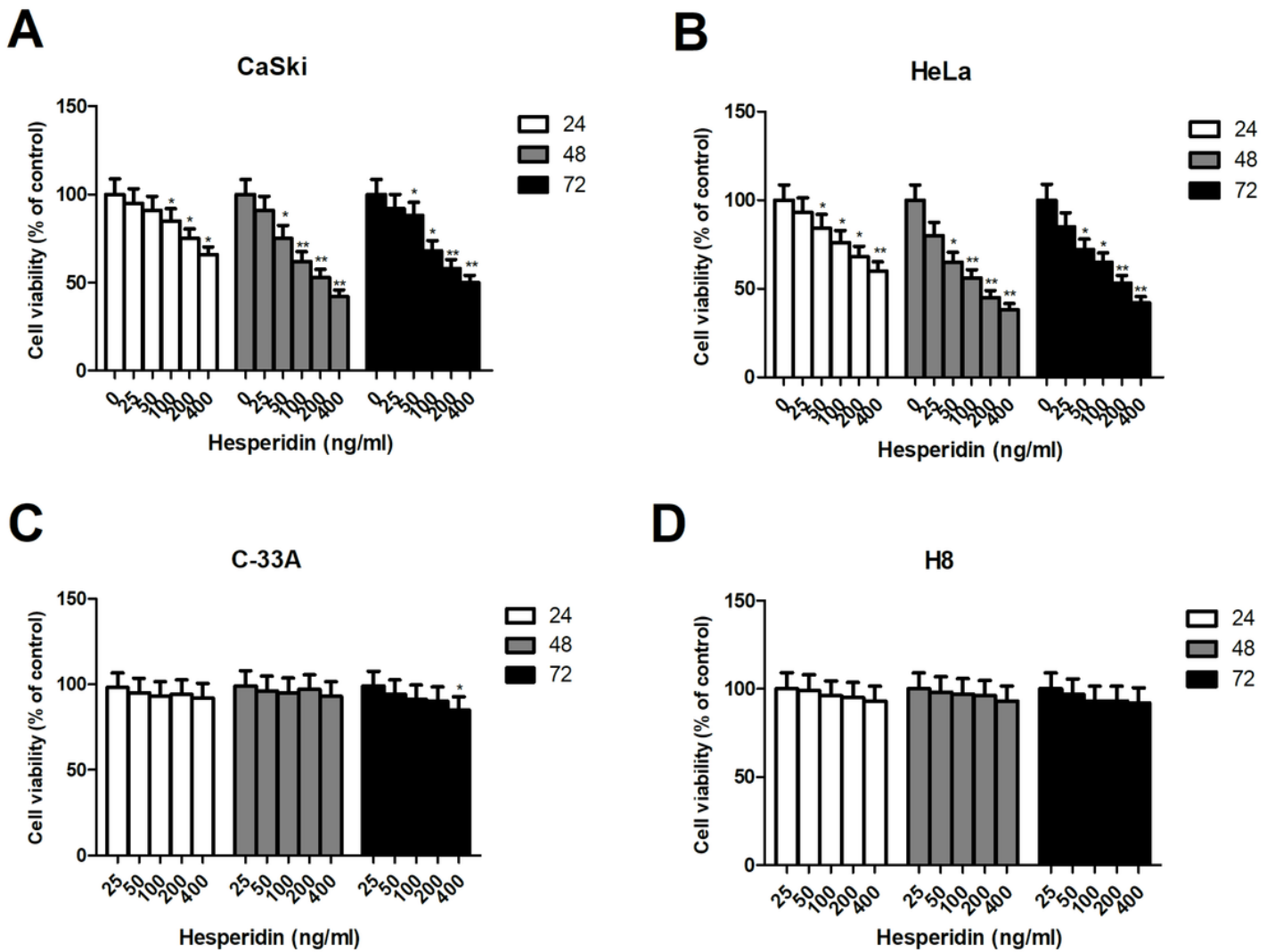


Figure 1

The effects of Hesperidin on the cell viability of cervical cancer cells and normal cervix epithelial cells evaluated by MTT assay. a The effects of Hesperidin on the cell viability of CaSki cells. b The effects of Hesperidin on the cell viability of HeLa cells. c The effects of Hesperidin on the cell viability of C-33A cells. d The effects of Hesperidin on the cell viability of H8 cells. Data were shown as the mean \pm SD of three determinations. *P<0.05, **P<0.01 vs. control.

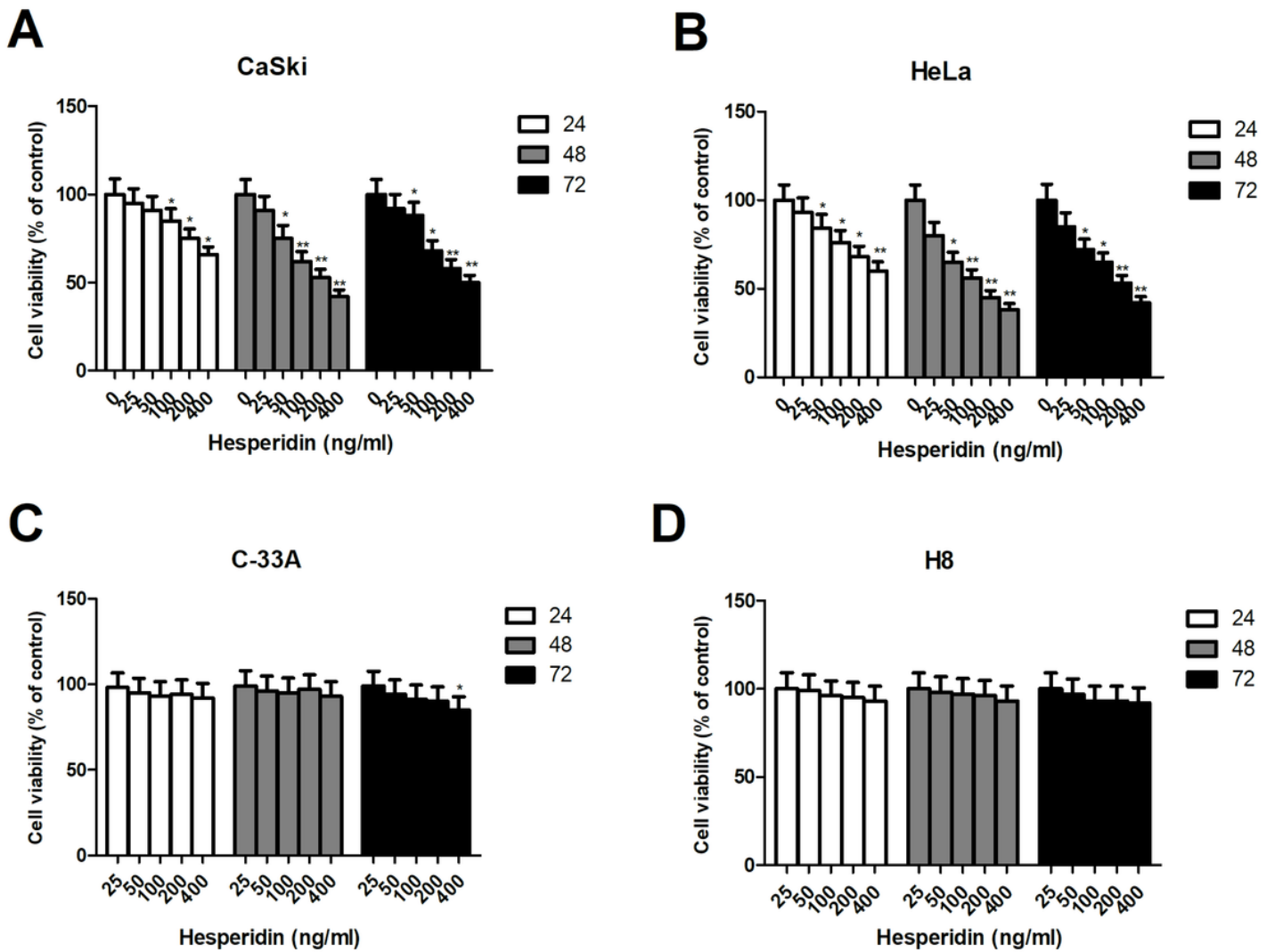


Figure 1

The effects of Hesperidin on the cell viability of cervical cancer cells and normal cervix epithelial cells evaluated by MTT assay. a The effects of Hesperidin on the cell viability of CaSki cells. b The effects of Hesperidin on the cell viability of HeLa cells. c The effects of Hesperidin on the cell viability of C-33A cells. d The effects of Hesperidin on the cell viability of H8 cells. Data were shown as the mean \pm SD of three determinations. * $P < 0.05$, ** $P < 0.01$ vs. control.

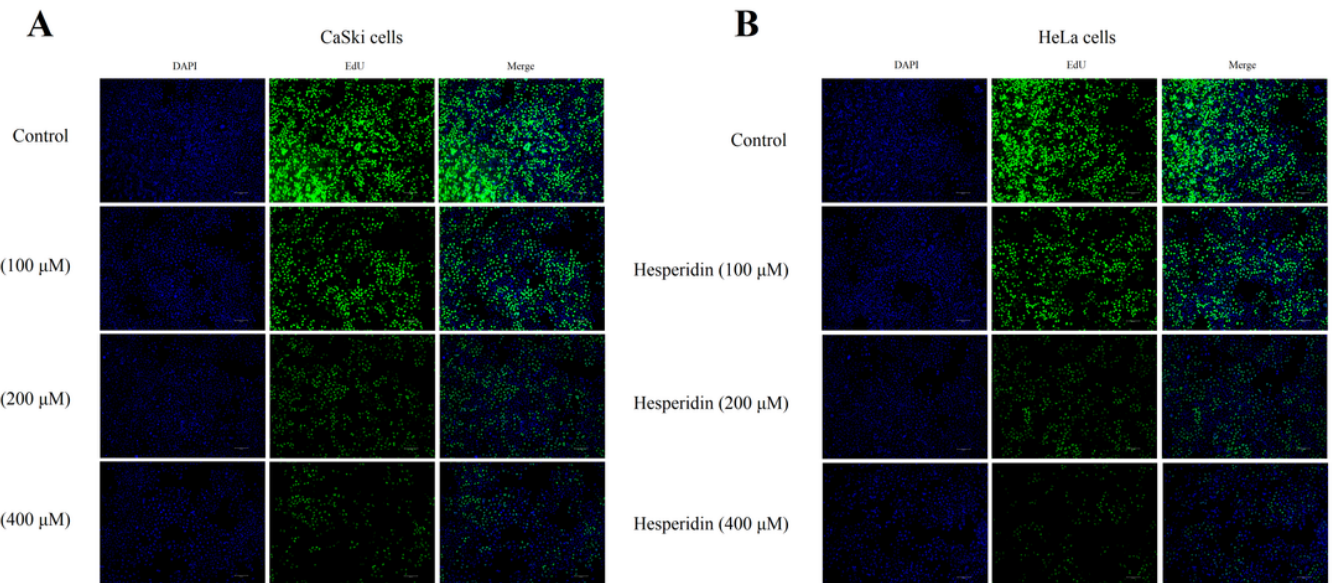


Figure 2

The effects of Hesperidin on the proliferation of CaSki and HeLa cells evaluated by EdU incorporation assay. a The effects of Hesperidin on the proliferation of CaSki cells. b The effects of Hesperidin on the proliferation of HeLa cells.

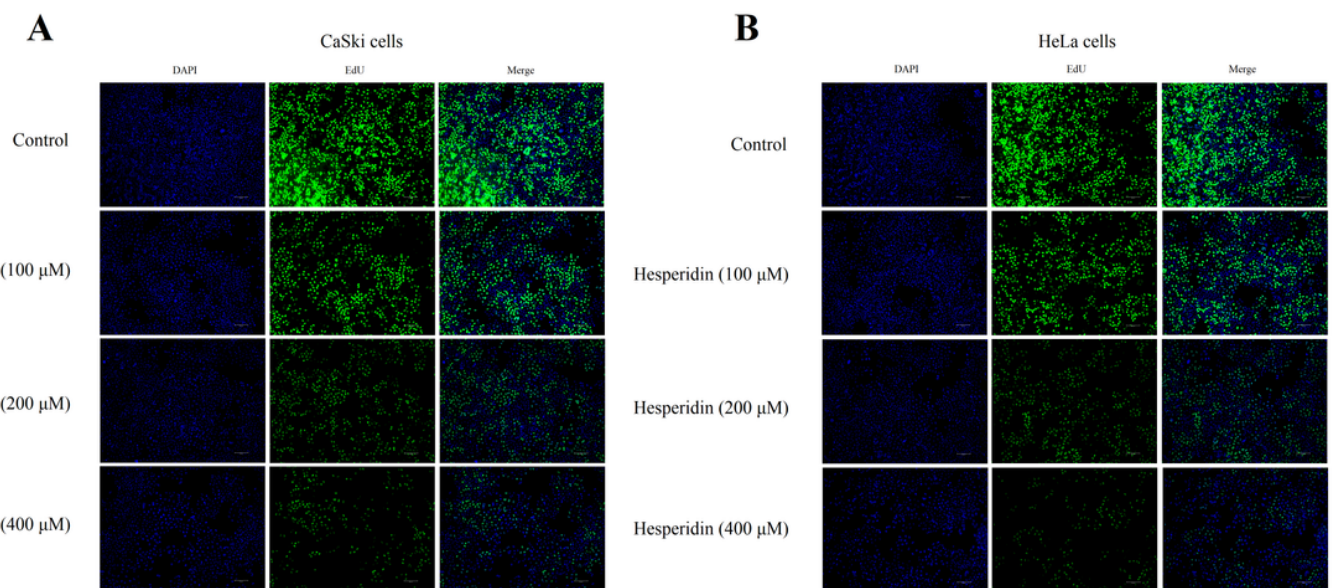


Figure 2

The effects of Hesperidin on the proliferation of CaSki and HeLa cells evaluated by EdU incorporation assay. a The effects of Hesperidin on the proliferation of CaSki cells. b The effects of Hesperidin on the proliferation of HeLa cells.

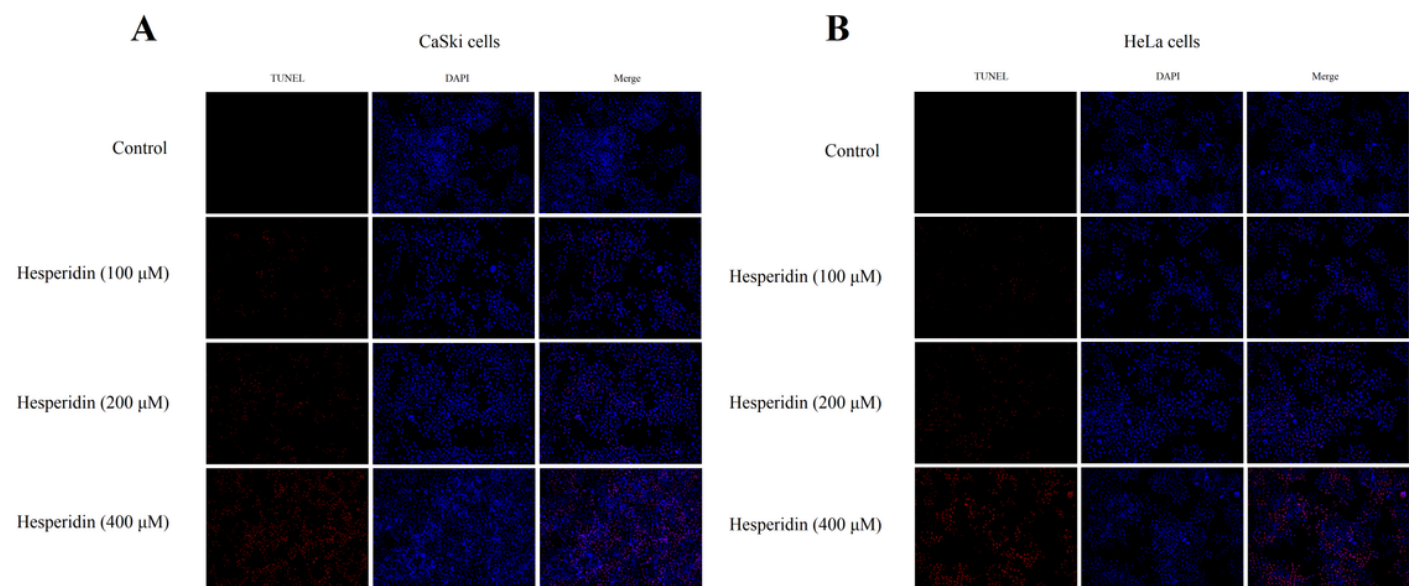


Figure 3

The effects of Hesperidin on the apoptosis of CaSki and HeLa cells evaluated by TUNEL assay. a The effects of Hesperidin on the apoptosis of CaSki cells. b The effects of Hesperidin on the apoptosis of HeLa cells.

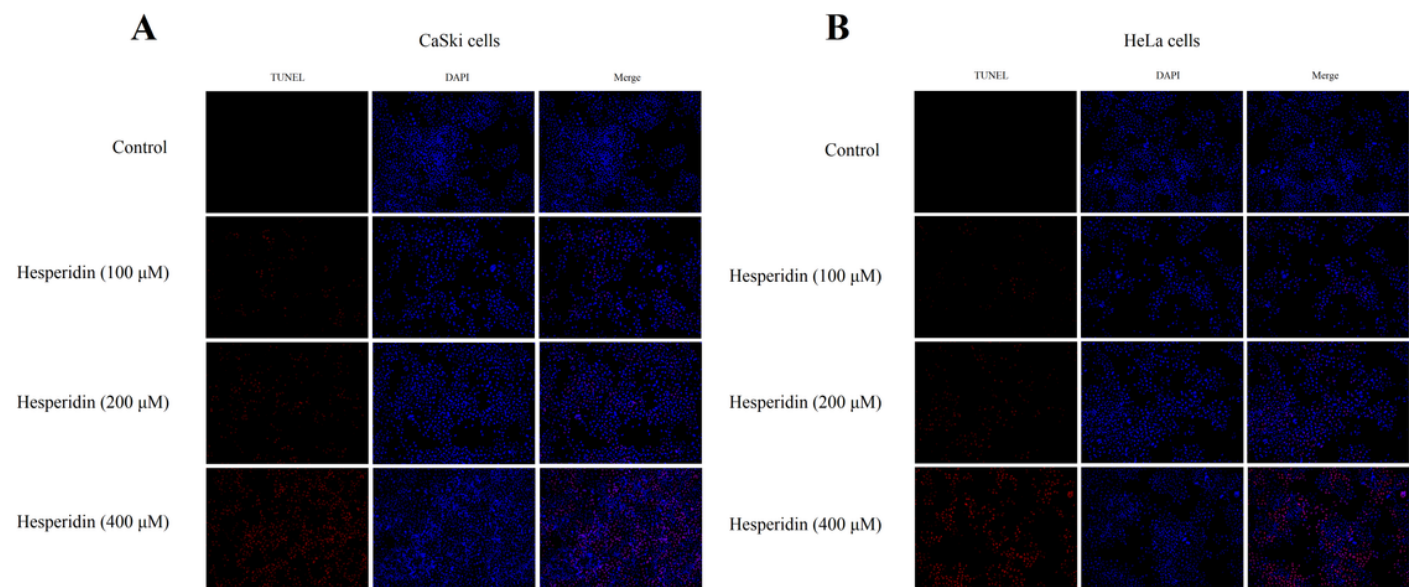


Figure 3

The effects of Hesperidin on the apoptosis of CaSki and HeLa cells evaluated by TUNEL assay. a The effects of Hesperidin on the apoptosis of CaSki cells. b The effects of Hesperidin on the apoptosis of HeLa cells.

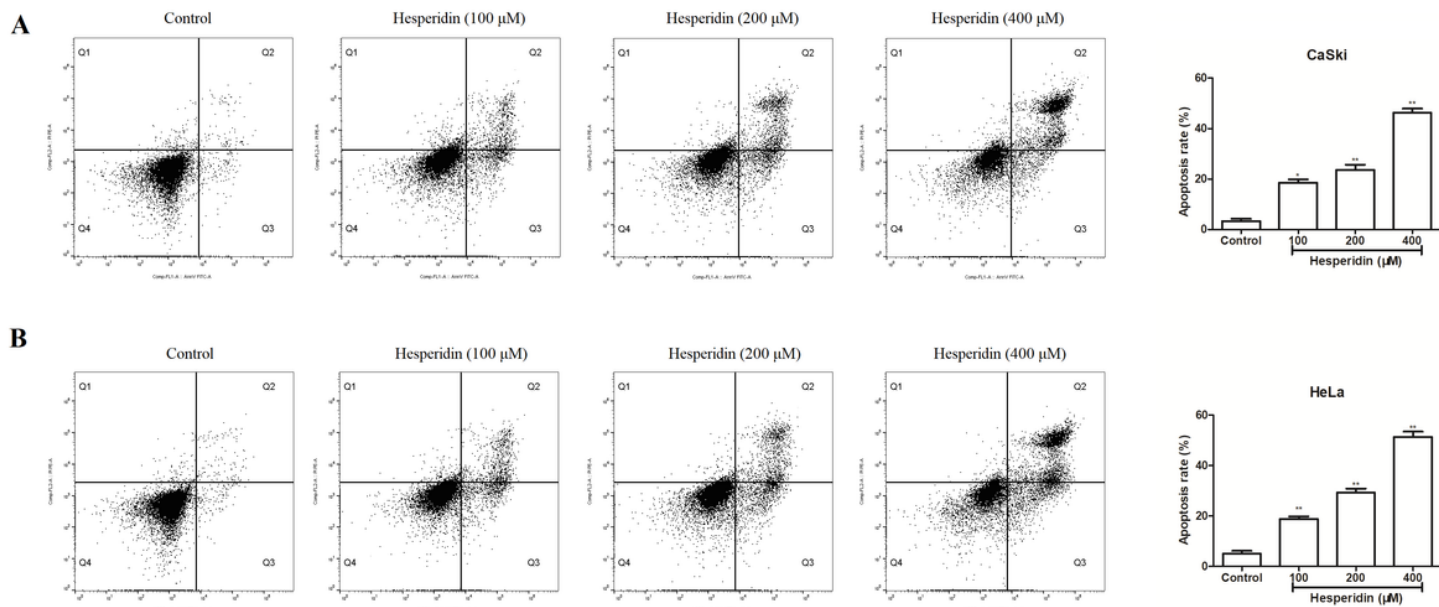


Figure 4

The effects of Hesperidin on the apoptosis of CaSki and HeLa cells evaluated by Annexin V-FITC/PI double staining on flow cytometry. a The effects of Hesperidin on the apoptosis of CaSki cells. b The effects of Hesperidin on the apoptosis of HeLa cells. Data were shown as the mean \pm SD of three determinations. * $P < 0.05$, ** $P < 0.01$ vs. control.

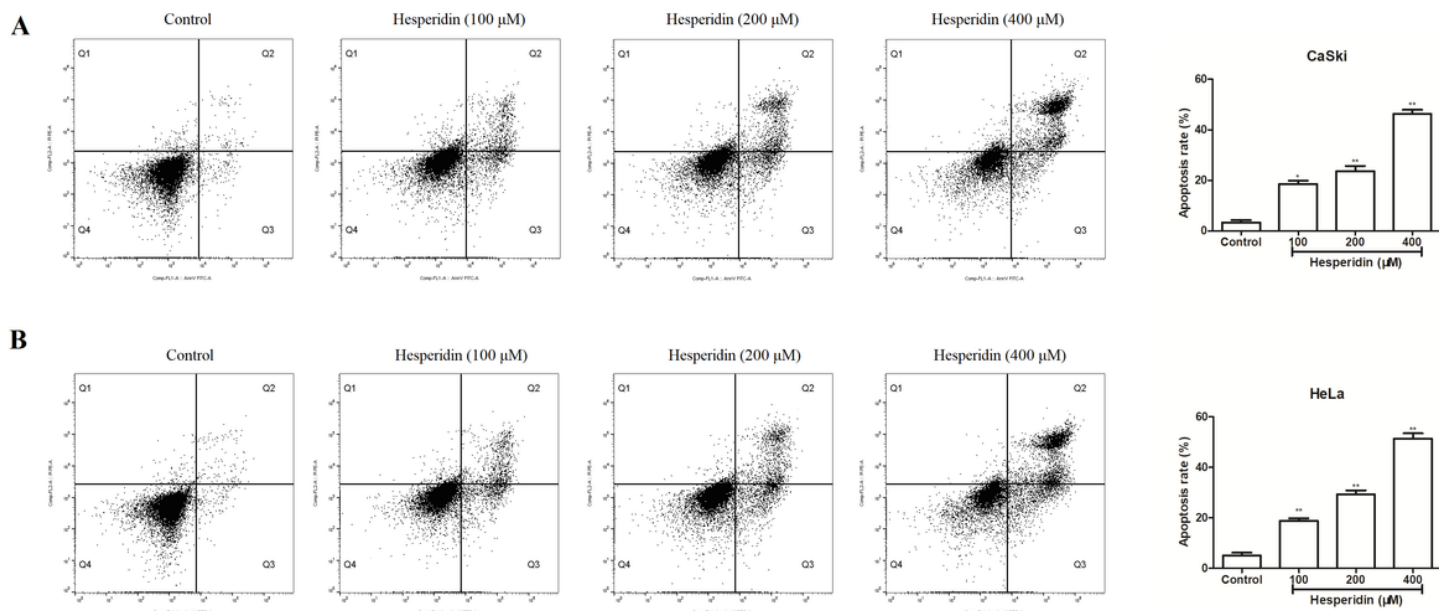


Figure 4

The effects of Hesperidin on the apoptosis of CaSki and HeLa cells evaluated by Annexin V-FITC/PI double staining on flow cytometry. a The effects of Hesperidin on the apoptosis of CaSki cells. b The effects of Hesperidin on the apoptosis of HeLa cells. Data were shown as the mean \pm SD of three determinations. * $P < 0.05$, ** $P < 0.01$ vs. control.

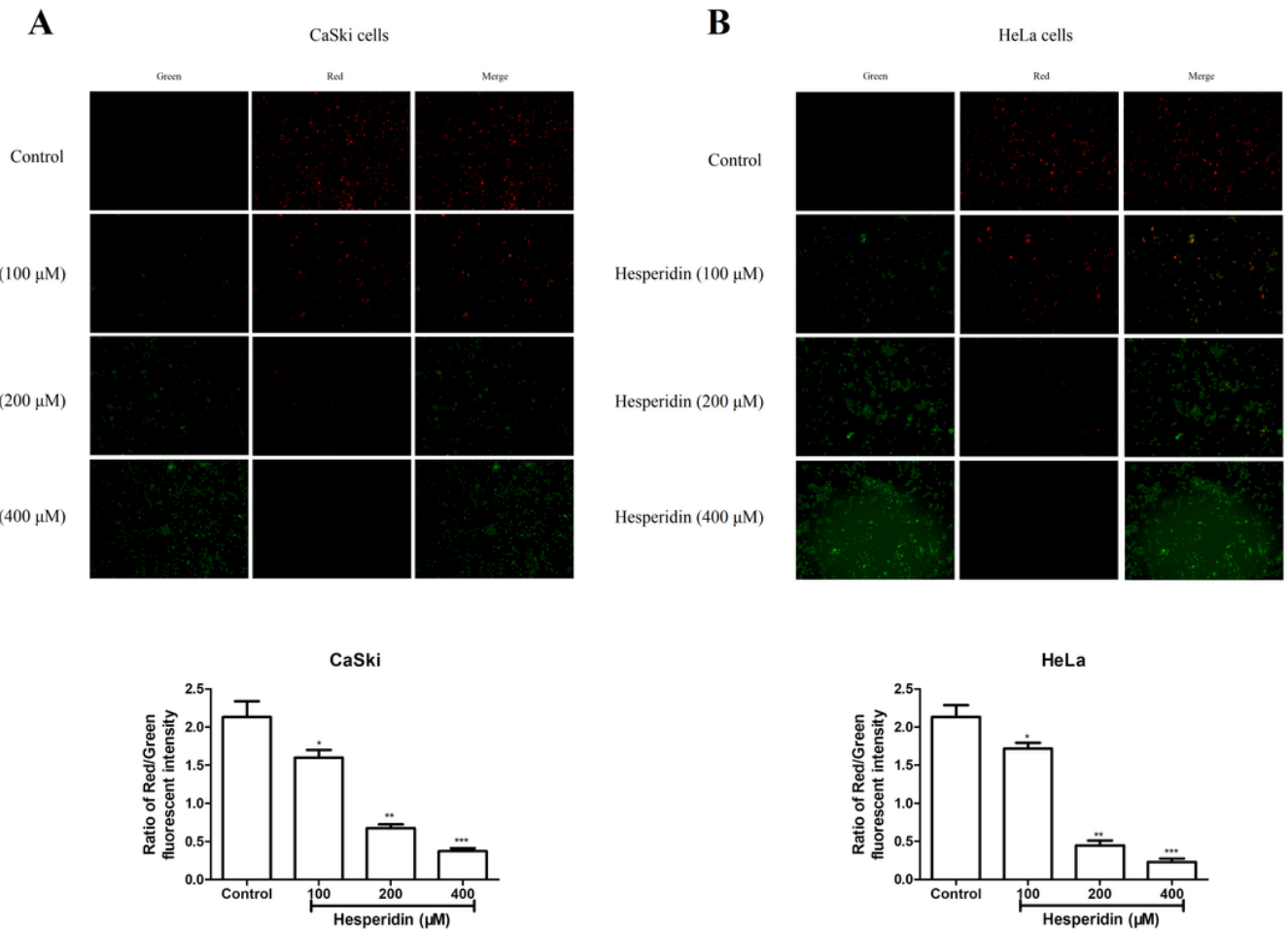


Figure 5

The effects of Hesperidin on the change of mitochondrial membrane potential in CaSki and HeLa cells evaluated by JC-1 staining and flow cytometry. a The effects of Hesperidin on the change of mitochondrial membrane potential in CaSki cells. b The effects of Hesperidin on the change of mitochondrial membrane potential in HeLa cells. Data were shown as the mean \pm SD of three determinations. * $P < 0.05$, ** $P < 0.01$, *** $P < 0.001$ vs. control.

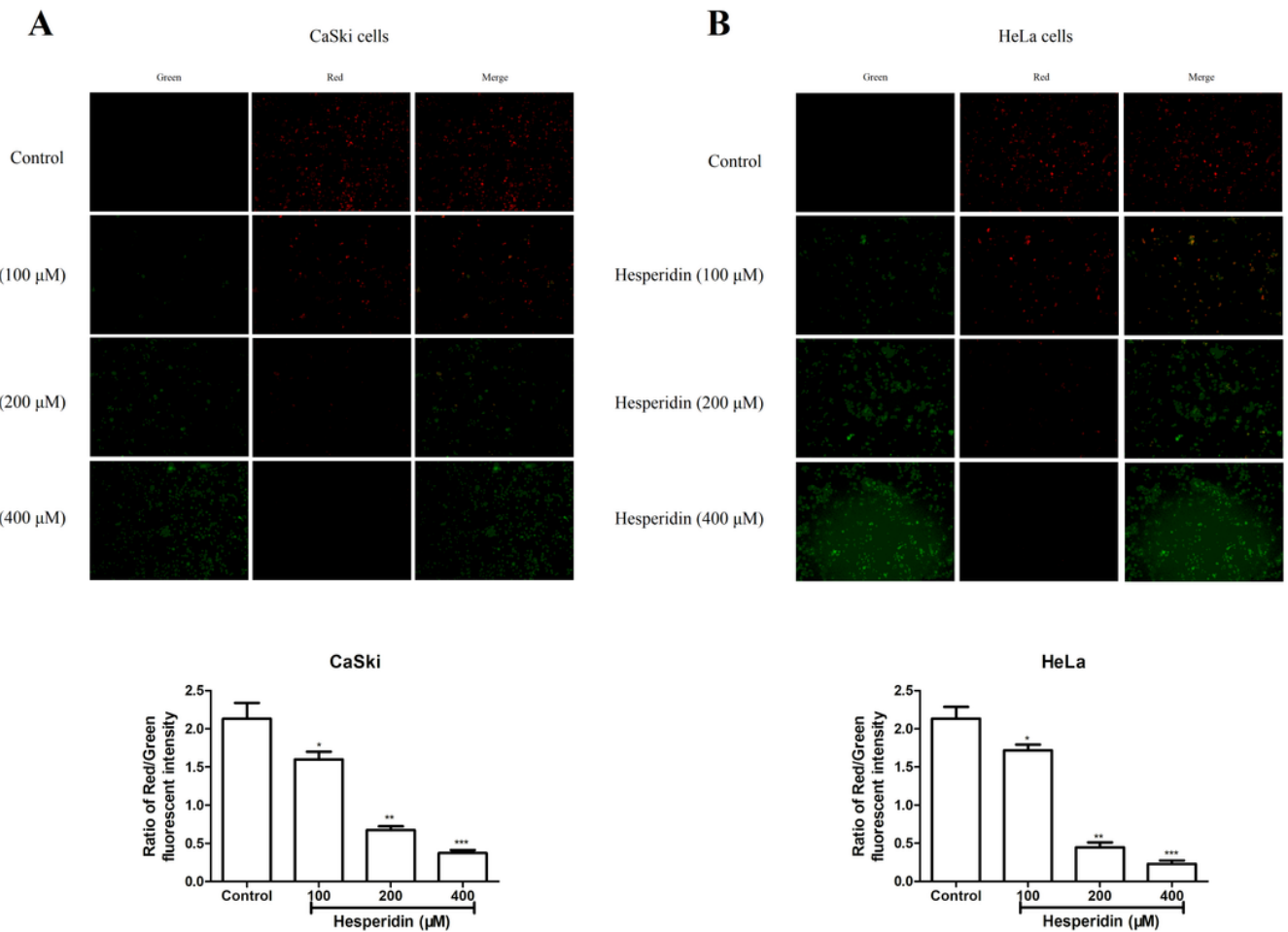


Figure 5

The effects of Hesperidin on the change of mitochondrial membrane potential in CaSki and HeLa cells evaluated by JC-1 staining and flow cytometry. a The effects of Hesperidin on the change of mitochondrial membrane potential in CaSki cells. b The effects of Hesperidin on the change of mitochondrial membrane potential in HeLa cells. Data were shown as the mean \pm SD of three determinations. * $P < 0.05$, ** $P < 0.01$, *** $P < 0.001$ vs. control.

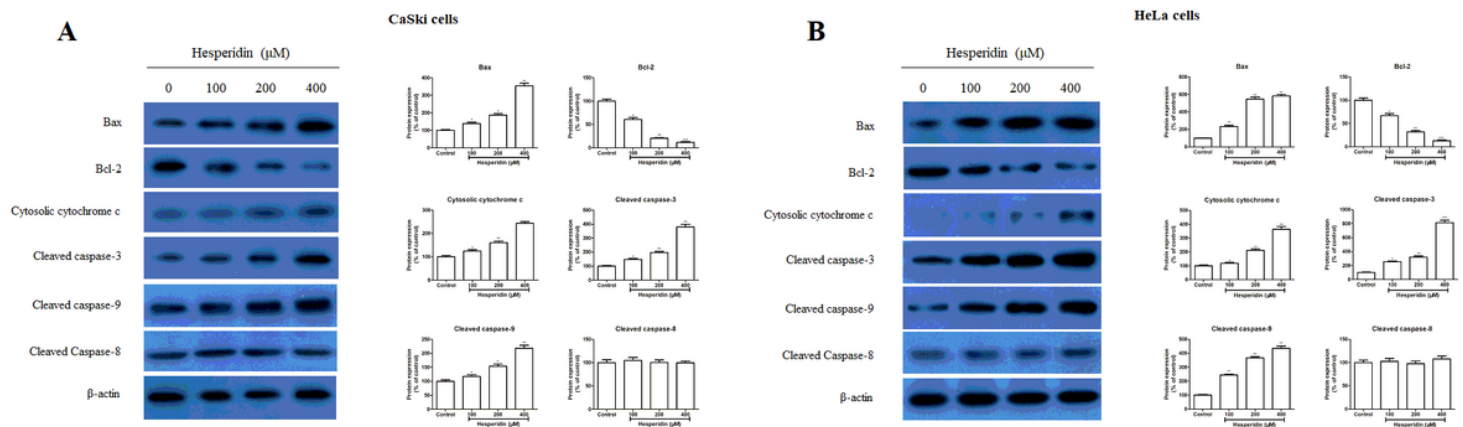


Figure 6

The effects of Hesperidin on the protein expression of cytosolic cytochrome c, Bax, Bcl-2, cleaved caspase-3, cleaved caspase-8, and cleaved caspase-9 in CaSki and HeLa cells evaluated by Western blotting. a The effects of Hesperidin on the protein expression of cytosolic cytochrome c, Bax, Bcl-2, cleaved caspase-3, cleaved caspase-8, and cleaved caspase-9 in CaSki cells. b The effects of Hesperidin on the protein expression of cytosolic cytochrome c, Bax, Bcl-2, cleaved caspase-3, cleaved caspase-8, and cleaved caspase-9 in HeLa cells. Data were shown as the mean \pm SD of three determinations. *P<0.05, **P<0.01, ***P<0.001 vs. control.

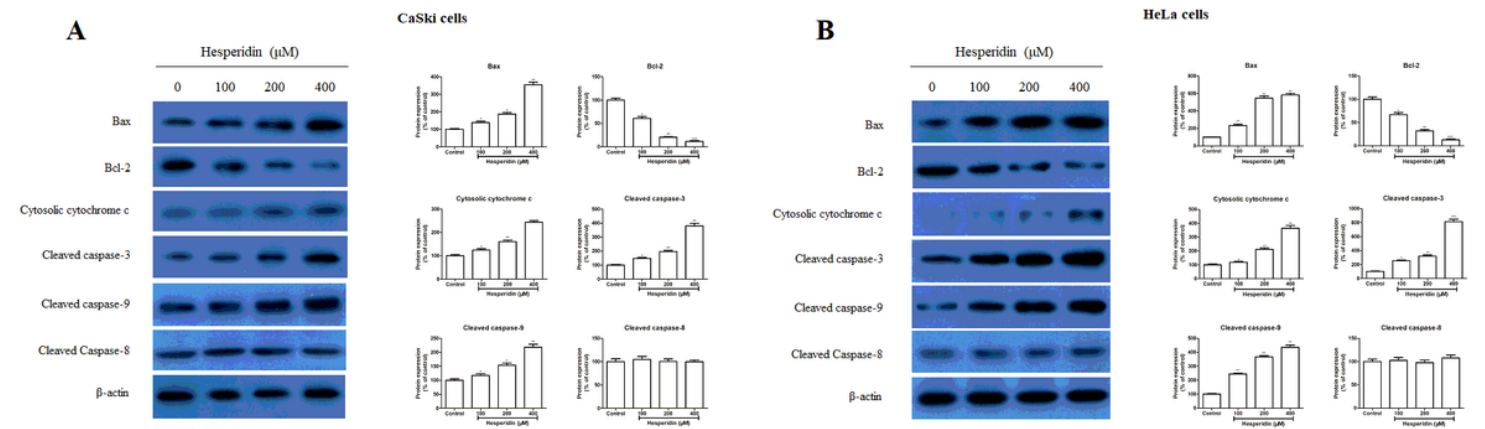
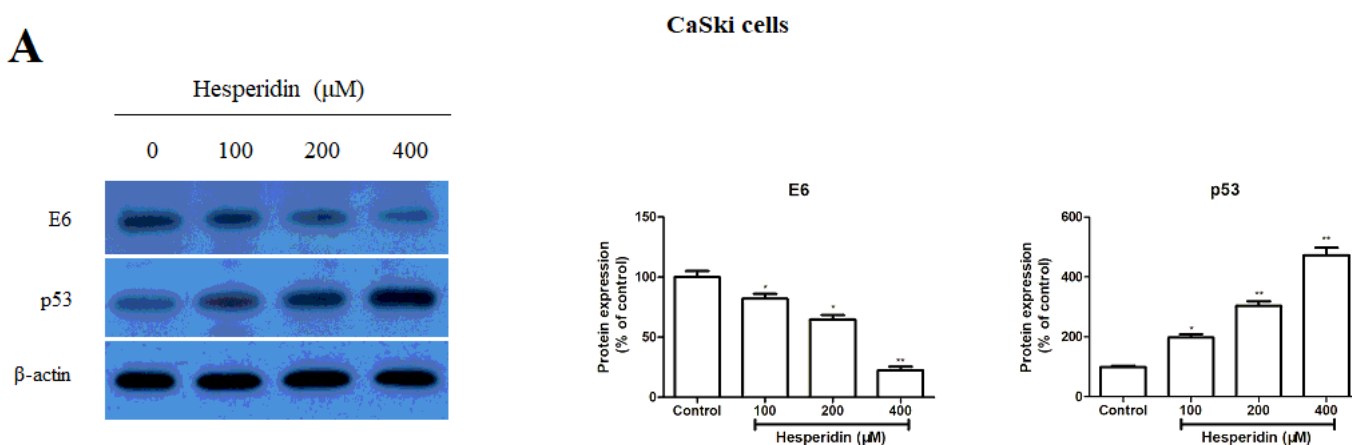
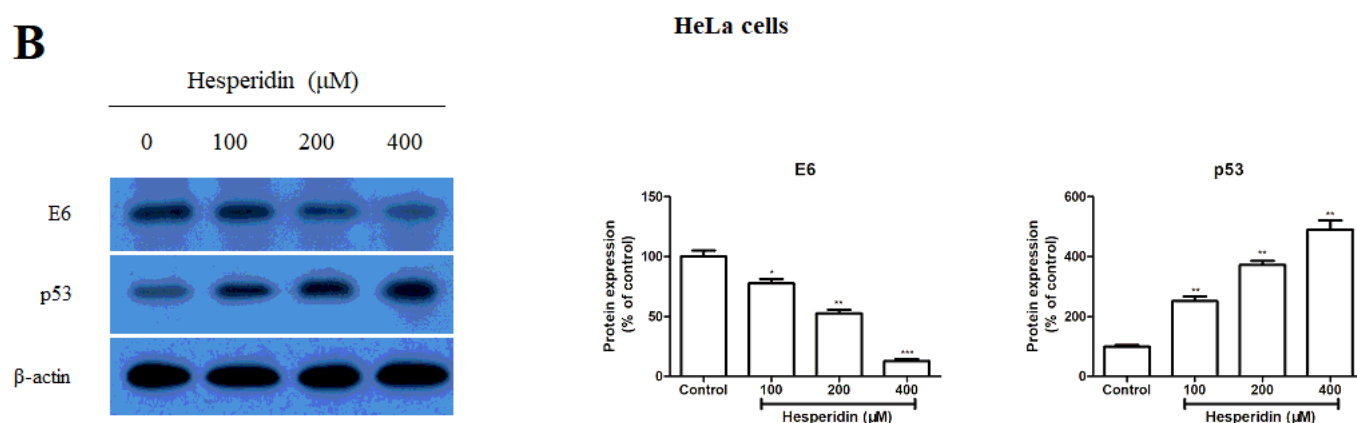
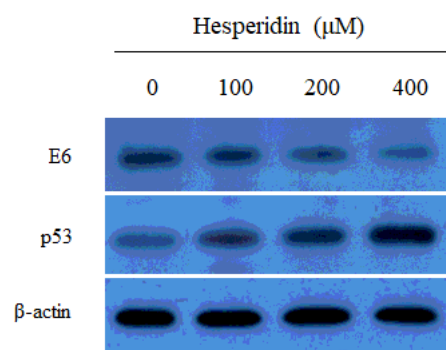
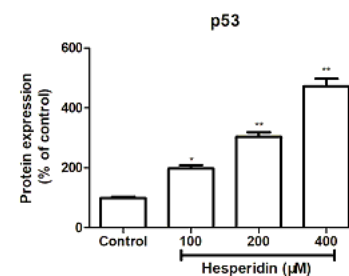
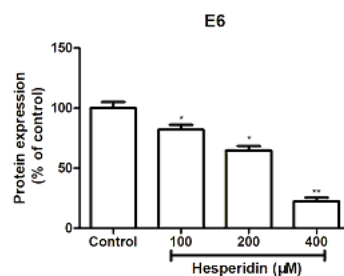
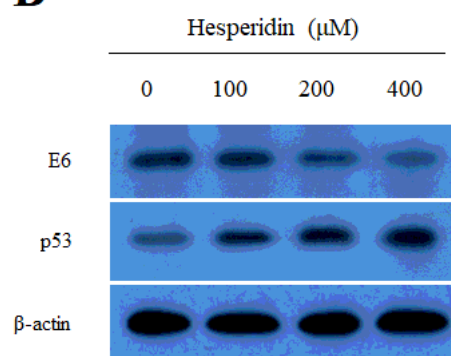
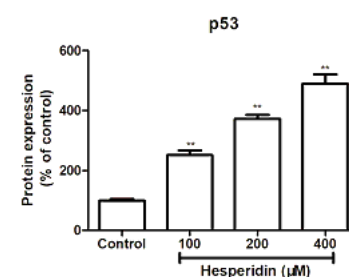
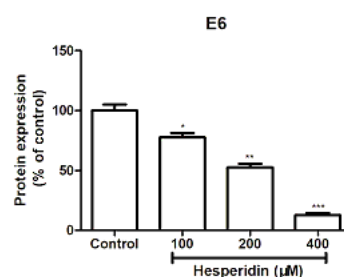


Figure 6

The effects of Hesperidin on the protein expression of cytosolic cytochrome c, Bax, Bcl-2, cleaved caspase-3, cleaved caspase-8, and cleaved caspase-9 in CaSki and HeLa cells evaluated by Western blotting. a The effects of Hesperidin on the protein expression of cytosolic cytochrome c, Bax, Bcl-2, cleaved caspase-3, cleaved caspase-8, and cleaved caspase-9 in CaSki cells. b The effects of Hesperidin on the protein expression of cytosolic cytochrome c, Bax, Bcl-2, cleaved caspase-3, cleaved caspase-8, and cleaved caspase-9 in HeLa cells. Data were shown as the mean \pm SD of three determinations. *P<0.05, **P<0.01, ***P<0.001 vs. control.

A**B****Figure 7**

The effects of Hesperidin on the protein expression of E6 and p53 in CaSki and HeLa cells evaluated by Western blotting. a The effects of Hesperidin on the protein expression of E6 and p53 in CaSki cells. b The effects of Hesperidin on the protein expression of E6 and p53 in HeLa cells. Data were shown as the mean \pm SD of three determinations. * $p < 0.05$, ** $p < 0.01$ vs. control.

A**CaSki cells****B****HeLa cells****Figure 7**

The effects of Hesperidin on the protein expression of E6 and p53 in CaSki and HeLa cells evaluated by Western blotting. a The effects of Hesperidin on the protein expression of E6 and p53 in CaSki cells. b The effects of Hesperidin on the protein expression of E6 and p53 in HeLa cells. Data were shown as the mean \pm SD of three determinations. * $p < 0.05$, ** $p < 0.01$ vs. control.